EMITTANCE GROWTH FROM MODULATED FOCUSING IN BUNCHED BEAM COOLING

M.Blaskiewicz*
BNL, Upton, NY 11973, USA

Abstract

The low energy RHIC electron cooling (LEReC) project at Brookhaven employs a linac to supply electrons with kinetic energies from 1.6 to 2.6 MeV. Along with cooling the stored ion beam the electron bunches create a coherent space charge field which can cause emittance growth. This is the primary source of heating when the cooling is well tuned. An analytic theory of this process is presented and compared with simulations.

INTRODUCTION

The low energy RHIC electron cooling project is currently under construction at BNL. The goal is to improve RHIC luminosity at very low energies, aiding in the study of the equation of state of the quark-gluon plasma near its phase boundary. We are using an electron linac with bunch lengths of a few centimeters to cool gold beams with lengths of several meters. Figure 1 shows the relative scale of the electron and ion bunches. Previous work [1] has shown one

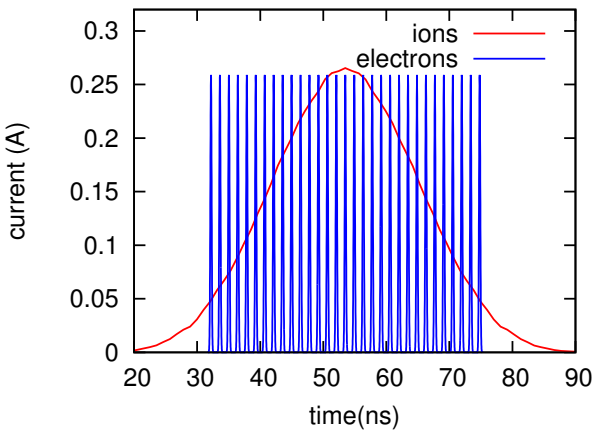

Figure 1: Longitudinal bunch structure for ions and electrons during cooling.

needs stable relative timing of the electron and ion bunches to avoid transverse heating of the ions. When the timing is stable the dominant ion heating mechanism is due to a combination of the space charge force from the electrons with the longitudinal intrabeam scattering (IBS) of the ions [2]. The idea is that longitudinal IBS causes the longitudinal action, and hence the synchrotron frequency, to vary. As the synchrotron tune varies the ions cross a variety of synchrobetatron resonances driven by the bunch structure of the electron beam resulting in emittance growth. Figure 2 shows qualitative simulations of the beam emittance for early times and Figure 3 shows a more extensive simulation.

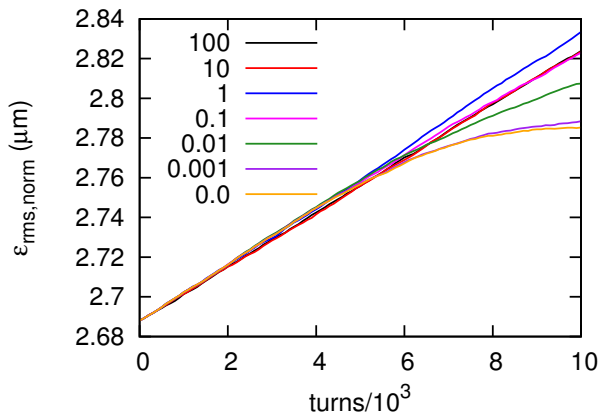

Figure 2: Emittance growth with electron bunches of 10 times nominal charge for a range of longitudinal IBS rates. The nominal IBS growth time is 650 seconds, labeled by 1. The labels are proportional to the rates, and saturation occurs for the nominal rate and faster rates.

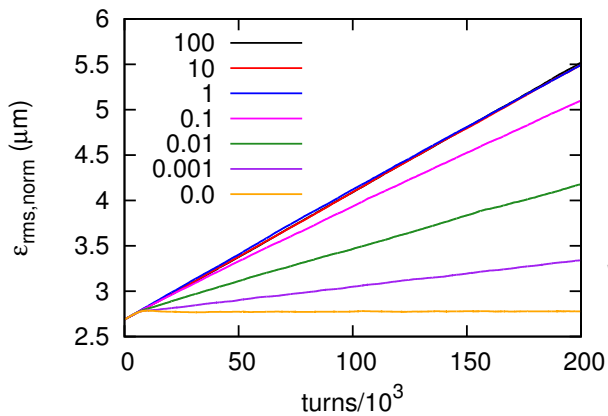

Figure 3: Emittance growth with electron bunches of 10 times nominal charge for a range of longitudinal IBS rates. This is an extended plot of the simulations in Figure 2

For the first few thousand turns IBS rates from zero through 100 times the nominal rate all yield the same rms emittance growth. After that the emittance growth rate depends weakly on the IBS rate. This effect as well as the detailed dependence of early emittance growth on various dynamical parameters can be explained.

* Work supported by the US Department of Energy under contract number DE-SC0012704

THEORY

Simulations have shown that only a single transverse dimension is needed so we consider the Hamiltonian

$$H(x,p) = \frac{Q_x}{2}\left(p^2+x^2\right) + \delta_p(\theta)a^2\Delta\psi_x(\tau)\ln\left(1+\frac{x^2}{a^2}\right), \quad (1)$$

where we use azimuth θ as the time-like variable, a is the nominal radius of the electron beam, $\tau = \tau(\theta)$ is the arrival time of the ion relative to the synchronous particle, x and p are the transverse position and momentum variables, $\Delta\psi_x(\tau)$ is the space charge induced, betatron phase shift of the ions from the electrons, and

$$\delta_p(\theta) = \sum_{k=-\infty}^{\infty}\delta(\theta-2\pi k) = \sum_{m=0}^{\infty}\frac{\cos(m\theta)}{(1+\delta_{m,0})\pi},$$

where $\delta_{m,0}$ is the Kronecker delta. First we use action angle variables with $x = \sqrt{2J}\cos\psi$, $p = -\sqrt{2J}\sin\psi$ yielding.

$$H(\psi,J) = Q_xJ + \delta_p(\theta)a^2\Delta\psi_x(\tau)\ln\left(1+\frac{2J\cos^2\psi}{a^2}\right) \quad (2)$$

$$= Q_xJ + \delta_p(\theta)\Delta\psi_x(\tau)\sum_{n=0}^{\infty}a_n(J)\cos(2n\psi). \quad (3)$$

For $n = 0$ we find [3]

$$a_0(J) = a^2\ln\left(\frac{1+J/a^2+\sqrt{1+2J/a^2}}{2}\right). \quad (4)$$

For $n > 0$

$$a_n(J) = \frac{-2a^2}{n}\left(\frac{-J/a^2}{1+J/a^2+\sqrt{1+2J/a^2}}\right)^n. \quad (5)$$

The detuning term in the Hamiltonian increases without bound as J increases but the change in tune will be quite small. The other terms $a_n(J)$ are bounded by $2a^2/n$ so the driving terms saturate with betatron amplitude. We will be examining resonant behavior with small driving terms so we consider a single betatron harmonic

$$H_1(\psi,J) = Q_xJ + \delta_p(\theta)\Delta\psi_x(\tau)a_n(J)\cos(2n\psi). \quad (6)$$

This Hamiltonian is straight forward to simulate but the delta function makes it difficult analytically.

To proceed take the slow approximation with

$$\delta_p(\theta)\cos(2n\psi) \approx \frac{\cos(2n\psi - p\theta)}{2\pi},$$

where p is chosen to minimize $|p-2nQ_x|$. Next do a scale transformation with $\Psi = 2n\psi - p\theta$. The action variable is unchanged. The new Hamiltonian is

$$H_2(\Psi,J) = (2nQ_x-p)J + 2n\Delta Q_xC(\tau)a_n(J)\cos\Psi, \quad (7)$$

where ΔQ_x is the maximum tune shift and $C(\tau)$ is the ratio of electron current to peak electron current. To solve (7) we define

$$\tilde{x} = \sqrt{2J}\cos\Psi, \quad \tilde{p} = -\sqrt{2J}\sin\Psi, \quad \delta = 2nQ_x - p.$$

Also let

$$\epsilon(J) = 2n\Delta Q_xa_n(J)/\sqrt{2J}.$$

With these definitions

$$H_2(\tilde{x},\tilde{p}) = \frac{\delta}{2}\left(\tilde{x}^2+\tilde{p}^2\right) + \tilde{x}C(\tau)\epsilon(J). \quad (8)$$

The equations of motion are

$$\frac{d\tilde{x}}{d\theta} = \frac{\partial H_2}{\partial\tilde{p}} = \delta\tilde{p} + \tilde{x}\tilde{p}\epsilon'(J)C(\tau) \quad (9)$$

$$\frac{d\tilde{p}}{d\theta} = -\frac{\partial H_2}{\partial\tilde{x}} = -\delta\tilde{x} - \epsilon(J)C(\tau) - \tilde{x}^2\epsilon'(J)C(\tau). \quad (10)$$

We will solve (9) and (10) approximately. The zeroeth order approximation is to ignore the terms proportional to $\tilde{x}\tilde{p}$ and $\tilde{x}^2$, and the first order approximation is to take $\tilde{x}^2 \approx J$. Note that J will evolve slowly for weak driving terms. Define $u = \tilde{p} + i\tilde{x}$ and approximate

$$\frac{du}{d\theta} = i\delta u - \alpha_qC(\tau), \quad (11)$$

where we allow for two approximations with $\alpha_0 = \epsilon(J_0)$ or $\alpha_1 = \epsilon(J_0) + J_0\epsilon'(J_0)$; J_0 is the initial value of J. To proceed we take

$$C(\tau) = \sum_{m=0}^{\infty}C_m(\hat{\tau})\cos(m\psi_s(\theta)), \quad (12)$$

where $\hat{\tau}$ is the synchrotron amplitude and ψ_s is the synchrotron phase. It is clear that the variation in $\hat{\tau}$ leads to changes in synchrotron frequency and subsequently the synchrotron phase, but the phase variations are bound to swamp any small variations in C_m. Hence we assume that $\hat{\tau}$ remains constant and that ψ_s is a random variable. Integrating (11) one gets

$$\Delta u = u(\theta) - u_0e^{i\delta\theta}$$

$$= -\int_0^{\theta}d\theta_1e^{i\delta(\theta-\theta_1)}\alpha_q\sum_{m=0}^{\infty}C_m(\hat{\tau})\cos(m\psi_{s,1}),$$

where $\psi_{s,1} = \psi_s(\theta_1)$. To characterize emittance growth note that u_0 is uncorrelated with Δu and take $< |\Delta u(\theta)|^2 >$ where angular brackets denote statistical averages,

$$< |\Delta u(\theta)|^2 > = \alpha_q^2\int_0^{\theta}d\theta_1\int_0^{\theta}d\theta_2e^{i\delta(\theta_2-\theta_1)}$$

$$\sum_{m,k}C_mC_k < \cos(m\psi_{s,1})\cos(k\psi_{s,2}) > . \quad (13)$$

Now we have

$$\psi_s(\theta) = \psi_s(0) + \int_0^\theta d\theta_1 Q_s(\theta_1),$$

where $\psi_s(0)$ is distributed uniformly on $[0, 2\pi)$ and $Q_s(\theta)$ is the time dependent synchrotron tune. We approximate the synchrotron tune as a stationary random variable. Averaging over $\psi_s(0)$ only the terms with $m = k$ survive. Define $\chi = \theta_2 - \theta_1$ so that

$$< |\Delta u(\theta)|^2 >= \alpha_q^2 \int_{-\theta}^{\theta} d\chi(\theta - |\chi|) e^{i\delta\chi}$$
$$\sum_{m=0}^{\infty} (1 + \delta_{m,0}) \frac{C_m^2}{2} < \cos[m \int_0^\chi Q_s(\chi_1) d\chi_1] > . \quad (14)$$

In (14) we need to evaluate the expectation value of the cosine term. The synchrotron tune varies over the IBS time which is much longer than any correlation time. Therefore the expectation value is totally dominated by fluctuations in the initial value of Q_s and is unaffected by any fluctuations in Q_s that occur on $[0, \chi]$. Additionally we will assume that Q_s is a gaussian random variable with mean $\bar{Q}_s$ and standard deviation σ_s. Then

$$< \cos[m \int_0^\chi Q_s(\chi_1) d\chi_1] >= \cos(m\bar{Q}_s\chi) e^{-m^2\sigma_s^2\chi^2/2}$$

The spread in synchrotron tune is typically $\gtrsim 1\%$ while IBS timescales are several minutes. For $m > 0$ the argument of the exponential will be very large for values of χ that are short compared to IBS timescales, verifying the previous assumption. This explains the behavior in Figure 2. For early times the emittance growth only depends on the initial variation in Q_s. After the resonant particles reach large amplitude they saturate and for the emittance to continue growing other particles must become resonant. This refreshing of the resonant reservoir is due to IBS. As long as the IBS is sufficiently fast the reservoir is always full and the growth in rms is steady.

For $\theta\sigma_s \gg 1$ and $\delta \neq 0$, $< |\Delta u(\theta)|^2 >$ grows linearly with θ

$$\frac{d < |\Delta u(\theta)|^2 >}{d\theta} \equiv < |\Delta u(\theta)|^2 >' = \alpha_q^2 \int_{-\infty}^{\infty} d\chi$$
$$\sum_{m=1}^{\infty} \frac{C_m^2}{2} \cos(m\bar{Q}_s\chi) e^{-m^2\sigma_s^2\chi^2/2 + i\delta\chi}. \quad (15)$$

Notice that the $m = 0$ term is absent in (15). This is because we assume $\delta \neq 0$. Otherwise the $m = 0$ term would grow as θ^2 and lead to unacceptable growth. The integrals in (15) over χ are straightforward and naturally break into two terms

$$< |\Delta u(\theta)|^2 >' = < |\Delta u(\theta)|_-^2 >' + < |\Delta u(\theta)|_+^2 >' \quad (16)$$

with

$$< |\Delta u(\theta)|_\pm^2 >' = \alpha_q^2 \sum_{m=1}^{\infty} \frac{\sqrt{2\pi} C_m^2}{4m\sigma_s} \exp\left(-\frac{1}{2}\left[\frac{m\bar{Q}_s \pm \delta}{m\sigma_s}\right]^2\right) \quad (17)$$

Equations (16) and (17) are the main results. To test them we will use $C(\tau) = 1/(1+\tau^2)$. With $\tau = \hat{\tau}\sin\psi_s$ only the even terms in equation (12) are nonzero. The fourier coefficients can be found in closed form [3]

$$C_{2m}(\hat{\tau}) = \frac{2}{(1 + \hat{\tau}^2/2)\sqrt{1 - z^2}} \left(\frac{1 - \sqrt{1 - z^2}}{z}\right)^{2m}, \quad (18)$$

where $z = \hat{\tau}^2/(2 + \hat{\tau}^2)$.

COMPARISON WITH SIMULATIONS

A code was written to simulate (6). To maximize resolution all the simulation particles start with the same values of J and $\hat{\tau}$. The synchrotron motion was modeled as a random process with the tunes modeled as identical, independently distributed gaussian processes updated once per turn

$$\bar{\psi}_s = \psi_s + 2\pi[\bar{Q}_s + q] \quad (19)$$
$$\bar{q} = rq + \sigma_s\sqrt{1 - r^2}n, \quad (20)$$

where $0 \leq r \leq 1$ defines the correlation time scale, n is a zero mean unit standard deviation gaussian deviate, and the overbars denote updated values.

The update for the thin lens kick of the electrons on the ions was done using a canonical transformation of Goldstein's 3rd type [4]. The initial variables are J, ψ and the updated variables are $\bar{J}, \bar{\psi}$ with generator $F(J, \bar{\psi}) = \Delta\psi_x(\tau) a_n(J) \cos(2n\bar{\psi})$

$$\bar{\psi} = \psi + \frac{\partial F(J, \bar{\psi})}{\partial J} \quad (21)$$
$$\bar{J} = J - \frac{\partial F(J, \bar{\psi})}{\partial \bar{\psi}}. \quad (22)$$

Equation (21) was solved iteratively with

$$\bar{\psi}_{n+1} = \psi + \Delta\psi_x(\tau) a_n'(J) \cos(2n\bar{\psi}_n)$$

and $\bar{\psi}_0 = \psi$. For our purposes $n = 5$ was completely adequate. Figure 4 shows initial and final transverse coordinates of a typical simulation and Figure 5 shows the rms emittance versus turn. We go on to compare these simulations with equations (16) and (17).

Figure 6 Shows growth rate from simulations for betatron harmonic $n = 2$ along with the analytic estimates and a simulation using the full Hamiltonian in equation (1). The only place a significant discrepancy exists is at the extreme left for small Q_x. Here the simulation using the full Hamiltonian appears to fix on a different resonance yielding a significantly larger growth rate. Other than that the techniques are all within a factor of 2. We go on to focus on the analytic

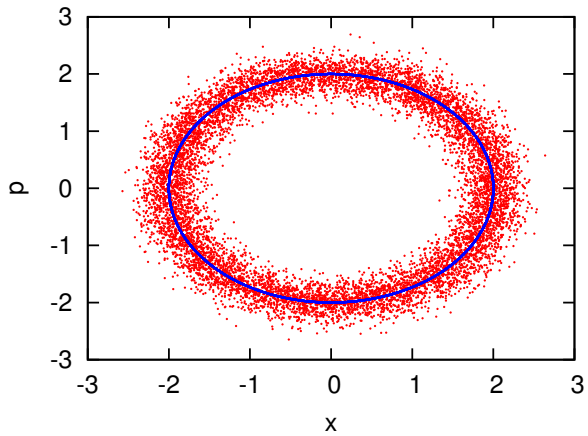

Figure 4: Initial (blue) and final (red) particle coordinates for a simulation with 10^4 particles.

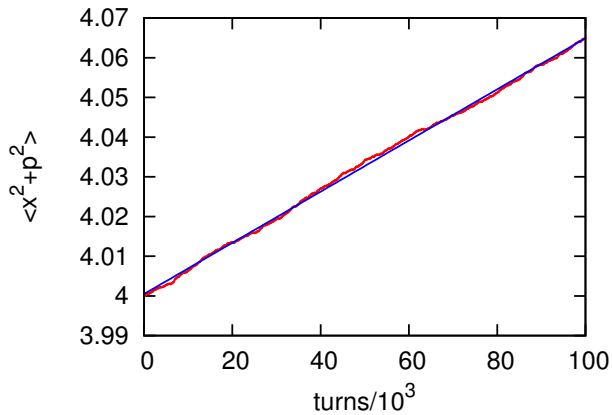

Figure 5: $< |u|^2 >$ versus time for a simulation with 10^5 particles and the same beam parameters as in Figure 4. The simulation data are in red and the blue line is a least squares fit. The slope of the line is the emittance growth and is to be compared with equations (16) and (17).

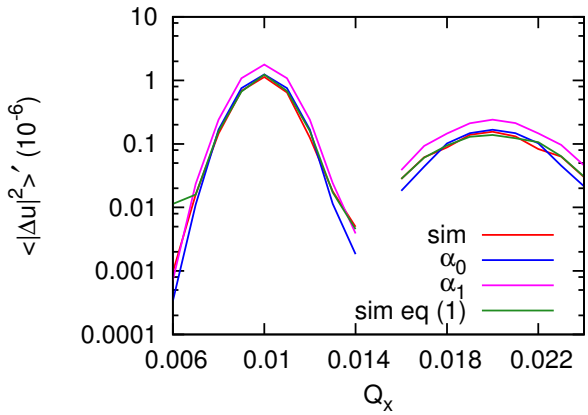

Figure 6: Emittance growth rates for $n = 1$, $J = 2a^2$, $\hat{\tau} = 3$ as a function of betatron tune. The formulas for α_0, α_1 and a simulation using the full Hamiltonian in eq (1) are also shown.

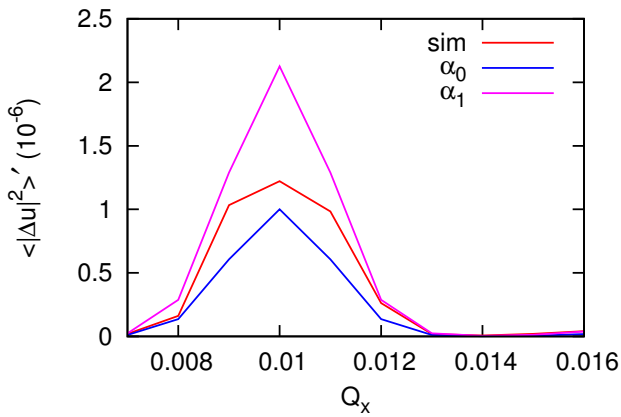

Figure 7: Emittance growth rates for $n = 1$, $J = a^2/2$, $\hat{\tau} = 3$ as a function of betatron tune. The formula for α_0 and α_1 bracket the simulation.

estimates and simulations using a single betatron harmonic. Figure 7 and 8 show results for betatron harmonic $n = 1$ with different values of synchrotron amplitude $\hat{\tau}$. Figure 9 shows growth as a function of $\hat{\tau}$ for $n = 2$ with other parameters fixed.For all these cases the betatron amplitude was fairly low. Figure 10 shows what can happen for betatron amplitudes large compared to the electron beam radius. In any case one can see that the formula and simulations give quantitatively comparable results so that equations (16) and (17) can be used for reliable factor of 2 estimates.

While the effect pointed out in this paper is relevant for LEReC it does not destroy cooling. Figures 11 and 12 show detailed simulations [2] of the transverse ion emittance versus time for a range of possible LEReC paramters with the nominal case being "A" for both. In general the cooling is reduced by still significant. Comparing case B with case A it might be advantagous to reduce the laser spot size reducing both emittance and bunch charge by the same factor.

ACKNOWLEDGMENT

This work followed from earlier unpublished work by Gang Wang and Vladimir Litvinenko. Thanks to Alexei Fedotov, Wolfram Fischer, Jorge Kewisch, Geoffrey Krafft (of JLAB) and Christoph Montag for useful discussions. Extra thanks to Wolfram Fischer for careful reading of the manuscript.

REFERENCES

[1] G. Wang C-A/AP/536, 2015.

[2] M. Blaskiewicz, J. Kewisch, C. Montag, in *Proc. COOL15*, JLAB, 2015.

[3] See 4.224.9 and 3.613.3 in Gradshteyn and Ryzhik *Table of Integrals Series and Products* academic press, 1980.

[4] H. Goldstein, *Classical Mechanics*, Addison Wesley, 1981.

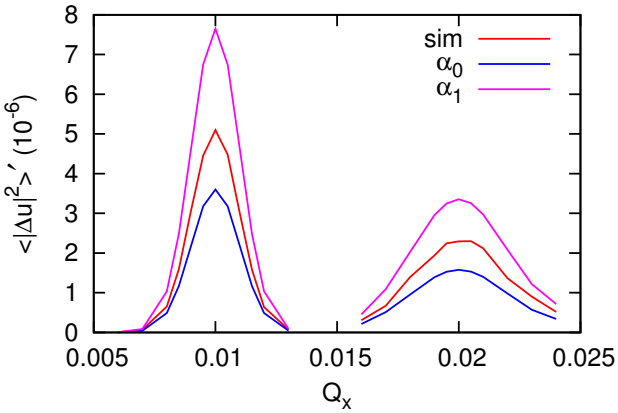

Figure 8: Emittance growth rates for $n = 1$, $J = a^2/2$, $\hat{\tau} = 30$ as a function of betatron tune. The formula for α_0 and α_1 bracket the simulation.

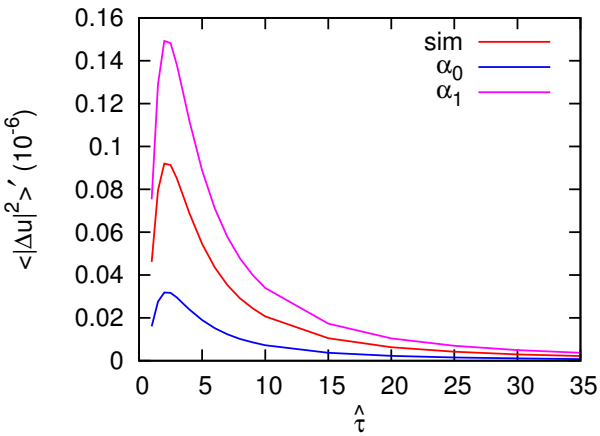

Figure 9: Emittance growth rates for $n = 2$, $J = a^2/2$ versus $\hat{\tau}$

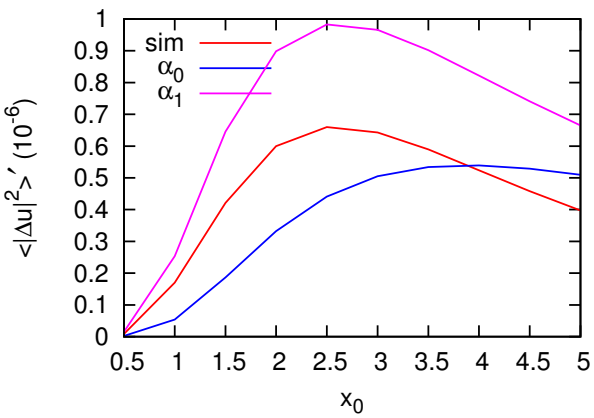

Figure 10: Emittance growth rates for $n = 2$, $\hat{\tau} = 30$ as a function of $x_0 = \sqrt{2J}/a$. For large betatron amplitudes the formulas overestimate the growth.

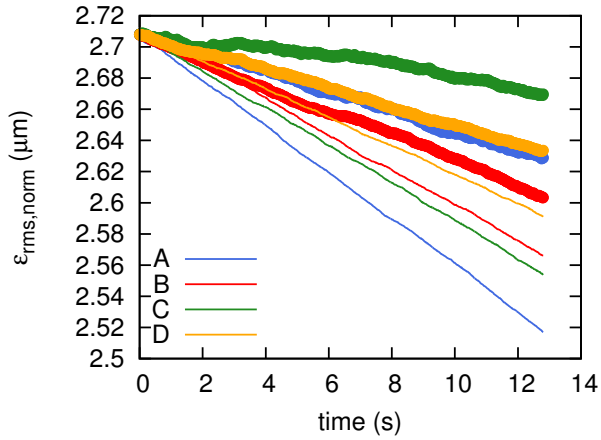

Figure 11: Ion emittance versus time for $\gamma = 4.1$. The thick lines show the predicted behavior while the thin lines neglect the coherent kicks from the electrons. There are four cases with different rms momentum spread σ_p, rms normalized emittance ϵ and electron bunch charge Q_e. The stated electron bunch charge was used for the coherent kick while the charge used for cooling was 30% less.
A, $\sigma_p = 4 \times 10^{-4}$, $\epsilon = 2$ μm, $Q_e = 130$ pC;
B, $\sigma_p = 4 \times 10^{-4}$, $\epsilon = 1$ μm, $Q_e = 65$ pC;
C, $\sigma_p = 8 \times 10^{-4}$, $\epsilon = 2$ μm, $Q_e = 130$ pC;
D, $\sigma_p = 8 \times 10^{-4}$, $\epsilon = 1$ μm, $Q_e = 65$ pC.

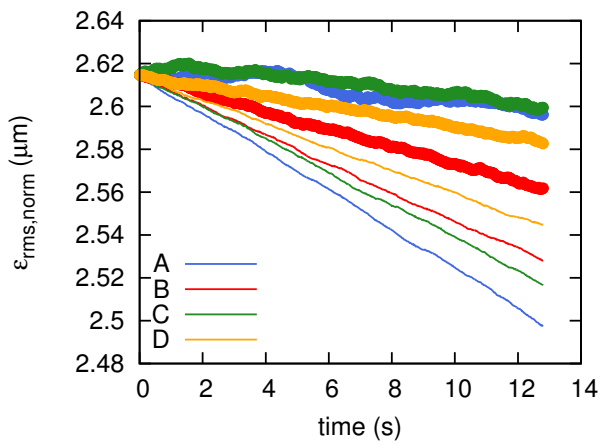

Figure 12: Ion emittance versus time for $\gamma = 6$. The thick lines show the predicted behavior while the thin lines neglect the coherent kicks from the electrons. There are four cases with different rms momentum spread σ_p, rms normalized emittance ϵ and electron bunch charge Q_e. The stated electron bunch charge was used for the coherent kick while the charge used for cooling was 30% less.
A, $\sigma_p = 4 \times 10^{-4}$, $\epsilon = 2$ μm, $Q_e = 156$ pC;
B, $\sigma_p = 4 \times 10^{-4}$, $\epsilon = 1$ μm, $Q_e = 78$ pC;
C, $\sigma_p = 8 \times 10^{-4}$, $\epsilon = 2$ μm, $Q_e = 156$ pC;
D, $\sigma_p = 8 \times 10^{-4}$, $\epsilon = 1$ μm, $Q_e = 78$ pC.